Nuclear spin-lattice relaxation in thallium-containing chalcogenide glasses

G. E. Jellison, Jr.* and S. G. Bishop
U. S. Naval Research Laboratory, Washington, D. C. 20375
(Received 18 August 1978)

NMR spin-lattice relaxation time (T_1) measurements for the two naturally abundant isotopes of thallium have been performed in two thallium-containing chalcogenide glasses as a function of temperature and frequency. The results for T_1 indicate that there are three regions of temperature dependence from 77 K to the glass-transition temperature. The relaxation in the high-temperature region is due to thallium-electron-thallium exchange. In the middle-temperature region, the relaxation is due to localized states, most likely the localized electronic states in the forbidden gap of amorphous semiconductors. The process responsible for the relaxation at low temperatures is probably the interaction of the thallium nuclei with disorder modes characteristic of amorphous materials.

I. INTRODUCTION

The existence of localized electronic states in the forbidden gap of amorphous semiconductors has been inferred from a variety of experimental studies of the optical and electronic properties of these materials.[1,2] In addition, several phenomenological models have been proposed to explain the physical origin and energy distribution of these states.[3-8] While the broad classification of amorphous or noncrystalline semiconducting solids is often employed, it is more appropriate to group these materials into several distinctly different categories on the basis, primarily, of their chemical bonding. Perhaps the most familiar categories are the tetrahedrally bonded amorphous group-IV semiconductors which can only be prepared by thin-film deposition, and the semiconducting chalcogenide glasses based on the group-VI elements. The experimental evidence concerning the localized electronic states in these two classes of noncrystalline semiconductors is sharply contrasted: unannealed evaporated films of amorphous Ge and Si exhibit substantial optical absorption within the forbidden gap and strong electron-spin-resonance (ESR) signals attributable to the presence of as many as 10^{20} cm^{-3} localized states[9,10]; on the other hand, pure chalcogenide glasses in bulk form usually exhibit no ESR under equilibrium (unilluminated) conditions, and only weak tails in the fundamental absorption edge, probably attributable to impurities, are observed.[1,2] In the case of the chalcogenide glasses, one must rely primarily on luminescence, transport, and optically induced ESR experiments to provide evidence for the existence of localized gap states.

In this paper we describe the application of nuclear-magnetic-resonance (NMR) techniques to the study of localized gap states in some chalcogenide glasses. Previous NMR studies of solid chalcogenide glasses[11-14] have dealt primarily with their structural properties and employed the wide-line NMR technique. The present study emphasizes pulsed NMR measurements of the temperature-dependent nuclear spin-lattice relaxation time which can be interpreted in terms of relaxation by localized electronic-gap states. Pulsed NMR measurements have previously been demonstrated to offer a powerful technique for the study of carrier localization in degenerate "liquid semiconductors."[15,16] In metals and highly conducting degenerate semiconductors the dominant magnetic relaxation process is usually the Korringa process in which nuclei couple to the spins of s-like conduction electrons through the Fermi contact or hyperfine interaction. However, in liquid semiconductors the magnetic spin-lattice relaxation rate is enhanced relative to the Korringa rate. This enhancement is a manifestation of the fact that the electron scattering becomes so strong that the electrons effectively remain longer near a given atom, i.e., they experience some degree of localization.[15,16] One would not expect the analysis of the relaxation process developed for liquid semiconductors in Refs. 15 and 16 to be applicable in solid amorphous semiconductors such as chalcogenide glasses, since the electrical conductivity is much lower and many of the carriers are highly localized. Two fundamentally important features of the NMR data reported here verify that the relaxation process in chalcogenide glasses cannot be characterized as the enhanced Korringa process observed in liquid semiconductors: (a) there exists a temperature range in which the spin-lattice relaxation time T_1 exhibits an exponential dependence upon reciprocal temperature with activation energy substantially less than $\frac{1}{2}E_g$, and (b) in this temperature range the relaxation process relies upon spin diffusion. The observed spin-diffusion process reveals that the relaxation mechanism is provided by localized centers, while the exponential temperature dependence, the

relatively small activation energy, and the magnitude of T_1, strongly indicate that these centers are thermally occupied localized electronic states. It should be emphasized that spin-lattice relaxation by such highly localized electronic states through the Fermi-contact interaction is a novel phenomenon which may be unique to amorphous semiconductors. Furthermore, it can be shown that under conditions where these thermally occupied localized states provide the dominant nuclear spin-lattice relaxation mechanism in an amorphous semiconductor, pulsed NMR techniques can be used to estimate the density of these localized gap states.

This paper is an extension of the work presented in Ref. 17, which reported in brief form the first observation of spin-lattice relaxation by localized gap states in a chalcogenide glass. Another glass $[Tl_2Se(2As_2Se_3)]$ is studied, and the other two regions of temperature dependence not treated in Ref. 17 are considered. In particular, it will be shown that the high-temperature nuclear relaxation is due to an exchange effect, while the relaxation in the low-temperature region is probably due to the interaction with low-lying disorder modes present in the glass. In addition, the details of the model calculation and the diffusion-constant calculation for the relaxation in the middle-temperature range are presented. Section II will present the relevant NMR theory, Sec. III will treat the spin-diffusion mechanism in these glasses, while the experimental details will be included in Sec. IV. The results will be presented in Sec.V, analyzed in Sec. VI, and discussed in Sec. VII. Section VIII is a summary of the paper.

II. RELEVANT NMR THEORY

Excellent texts exist on basic NMR theory (see Refs. 18–20), so only the necessary parts of the theory will be discussed briefly here. In particular, it will be assumed that the nuclear spin $I = \frac{1}{2}$ (both thallium isotopes have $I = \frac{1}{2}$).

In addition to the normal Zeeman coupling of the nuclear dipole moment to the applied magnetic field, we will consider nuclear dipole-dipole and electron-nuclear magnetic coupling. These additional interactions contribute to NMR line broadening and in certain circumstances to nuclear spin-lattice and spin-spin relaxation. The spin-lattice relaxation time T_1 is a measure of the rate at which the nuclear spin system transfers energy to the lattice, while the spin-spin relaxation time T_2 is a measure of the rate at which the spin system loses phase coherence. If more than one relaxation process is effective at a particular temperature over the entire sample, the relaxation rates are additive, i.e.,

$$1/T_1^{\text{tot}} = 1/T_1^{\text{I}} + 1/T_1^{\text{II}} + 1/T_1^{\text{III}} + \cdots . \tag{1}$$

The dipole-dipole interaction, which results from the magnetic coupling between nuclei, can be expressed as[19]

$$H_{dd} = (\gamma_1\gamma_2\hbar^2/r_{12}^3)\,(A + B + C + D + E + F)\,, \tag{2}$$

where γ_1, γ_2 are the gyromagnetic ratios of the two interacting nuclei, and r_{12} is the vector between these two nuclei. The quantities A–F are dependent upon θ, the angle between $\vec{r}_{12}$ and $\vec{H}_0$ (the applied magnetic field), and upon various spin operators (see Ref. 19). The term A is completely diagonal, while term B mixes $|\frac{1}{2}, -\frac{1}{2}\rangle$ with $|-\frac{1}{2}, \frac{1}{2}\rangle$ states (this is often called the mutual spin-flip operator).

The electron-nucleus magnetic interactions of interest can be subdivided into three categories: the chemical shift interaction, Fermi contact hyperfine interaction, and the nucleus-electron-nucleus indirect interaction. All three interactions can create line shape changes and nuclear relaxation.

The chemical shift is a tensorial interaction resulting from the magnetic coupling of electrons and the applied field; its Hamiltonian can be written phenomenologically as

$$H_{\text{cs}} = \vec{I}\cdot\ddot{A}_{\text{cs}}\cdot\vec{H}_0\,, \tag{3}$$

where $\ddot{A}_{\text{cs}}$ is the chemical-shift tensor. This interaction can be divided into two parts: a diamagnetic part[21] and a paramagnetic part.[22] The chemical-shift interaction will broaden the resonance absorption (the anisotropic part) and shift the resonant field with respect to the "bare" nucleus (the isotropic part); the size of the paramagnetic part (which results in a negative shift in field) is often correlated with the amount of covalency of interatomic bonding.[23]

The Fermi-contact hyperfine interaction results from a coupling between the s-like conduction electrons and the nuclei; its Hamiltonian can be expressed as[18,19,24]

$$H_{\text{Fc}} = \tfrac{8}{3}\pi\gamma_n\gamma_e\hbar^2\vec{I}\cdot\vec{S}\,\delta(\vec{r})\,, \tag{4}$$

where γ_e (γ_n) is the electronic (nuclear) gyromagnetic ratio, $\vec{S}$ ($\vec{I}$) is the electron (nuclear) spin vector, $\vec{r}$ is the vector between the nucleus and electron and δ is the Dirac delta function. Note that the interaction vanishes except at the nuclear site; therefore, only electrons that have a nonzero probability of being at the nuclear site may contribute to this interaction.

The nucleus-electron-nucleus indirect interac-

tion occurs through an admixture of the excited electronic states into the ground state, and its Hamiltonian can be written phenomenologically as

$$H_{\text{ind}} = \vec{I}_1 \cdot \vec{A}_{12} \cdot \vec{I}_2 . \tag{5}$$

Generally, this Hamiltonian can be divided into a diagonal part (called the exchange or scalar term), written[25]

$$H_{\text{ex}} = A_{12}\vec{I}_1 \cdot \vec{I}_2 = A_{12}[I_{1z}I_{2z} + \tfrac{1}{2}(I_1^+ I_2^- + I_1^- I_2^+)] , \tag{6}$$

and a traceless part, which is termed the pseudodipolar term, often approximated as[25]

$$H_{\text{pd}} = B_{12}(A + B + C + D + E + F) , \tag{7}$$

where the terms A–F are the same as in Eq. (2). It is found that the exchange interaction between *unlike* nuclei increases the second moment of the resonance line, whereas the exchange interaction between like nuclei does not.[25]

III. SPIN DIFFUSION

All of the interactions introduced in Sec. II can result in homogeneous relaxation over the entire sample. If, however, a small fraction of the sample volume relaxes with localized centers, the rest of the sample can relax by communicating with the nuclei in direct contact with a localized center via spin diffusion.

Spin diffusion occurs through the mutual spin flip of neighboring *like* nuclei.[18,26] The Zeeman Hamiltonian commutes with terms like $I_{1z}I_{2z}$ but does not commute with terms like $(I_1^+ I_2^- + I_1^- I_2^+)$. Therefore, there will be a mixing of $|\tfrac{1}{2}, -\tfrac{1}{2}\rangle$ with $|-\tfrac{1}{2}, \tfrac{1}{2}\rangle$, and the proper eigenfunctions are

$$\psi^S = (1/\sqrt{2})(|\tfrac{1}{2}, -\tfrac{1}{2}\rangle - |-\tfrac{1}{2}, \tfrac{1}{2}\rangle) \quad \text{(singlet)} , \tag{8}$$

and

$$\psi^T = (1/\sqrt{2})(|\tfrac{1}{2}, -\tfrac{1}{2}\rangle + |-\tfrac{1}{2}, \tfrac{1}{2}\rangle) \quad \text{(triplet)} .$$

The energy difference between the singlet and triplet states is given by

$$\hbar\omega_1 = E^T - E^S = \langle\psi^T|H|\psi^T\rangle - \langle\psi^S|H|\psi^S\rangle , \tag{9a}$$

where

$$H = H_{\text{Zeeman}} + H_{dd} + H_{\text{ind}} , \tag{9b}$$

which yields

$$\omega_1 = \frac{A_{12}}{\hbar} - \left(\frac{\gamma^2\hbar}{2\pi r_{12}^3} + \frac{B_{12}}{\hbar}\right)\left(\frac{1 - 3\cos^2\theta}{2}\right) . \tag{9c}$$

The contribution A_{12} comes from the exchange interaction [Eq. (6)], while the contributions

$$\frac{\gamma^2\hbar^2}{r_{12}^2}\left(\frac{1 - 3\cos^2\theta}{2}\right) \quad \text{and} \quad B_{12}\left(\frac{1 - 3\cos^2\theta}{2}\right)$$

come from the dipole-dipole interaction [Eq. (2)] and pseudodipolar interaction [Eq. (7)], respectively.

The above clearly represents an oversimplification, since we have only treated two spins, while the sample will have 10^{22} spins/cm^3. The other spins can be introduced by supposing that their effect is to give a certain width to the two levels, $|\tfrac{1}{2}, -\tfrac{1}{2}\rangle$ and $|-\tfrac{1}{2}, \tfrac{1}{2}\rangle$, of the pair considered. Using this assumption and Fermi's golden rule, we can get an approximate value of W, the probability per unit time for mutual spin flip,[18]

$$W = \tfrac{1}{8}\sqrt{\pi}\,\omega_1^2\langle\Delta\omega^2\rangle^{-1/2} , \tag{10}$$

where $\langle\Delta\omega^2\rangle$ is the second moment of the NMR absorption. It has been shown that this process obeys a diffusion equation, within certain limits, where the spin-diffusion constant D is given by[18]

$$D = Wa^2 , \tag{11}$$

a being the distance between nearest interacting nuclei, where the anisotropy of W has been neglected.

Note that Eq. (9c) includes contributions from the indirect interaction. Normally this is ignored, but, for the case of thallium which has 81 electrons/atom, it cannot be ignored, since its magnitude is about 15 times the dipolar interaction[25] and will tend to dominate. Therefore, spin diffusion will be dominated by the indirect interaction in thallium-containing materials, and D should be much larger in thallium-containing materials (for the thallium nuclei) than in solids which contain other much lighter nuclei.

In Ref. 25, it was shown that A_{12} decreases as $1/r_{12}^3$ for a metal, and exponentially with r_{12} for an insulator. From Eqs. (9)–(11), it follows that D will decrease as a is increased. Note that spin diffusion is an energy-conserving interaction, and therefore can occur only between like nuclei (^{205}Tl-^{203}Tl pairs cannot contribute to spin diffusion). The average distance between two ^{205}Tl nuclei will be less than the distance between two ^{203}Tl nuclei, since the natural abundance of ^{205}Tl is greater than the natural abundance of ^{203}Tl. Therefore

$$D(^{205}\text{Tl}) > D(^{203}\text{Tl}) . \tag{12}$$

This fact will help us later determine if a relaxation mechanism is dependent on spin diffusion, since $T_1(^{205}\text{Tl}) < T_1(^{203}\text{Tl})$ if spin diffusion is a limiting factor in spin-lattice relaxation. (All other possible factors, such as spin, gyromagnetic ratio, and chemical bonding are nearly identical for the two isotopes of thallium.)

The determination of D is a very difficult proposition, even in cubic crystals; in amorphous ma-

terials, an accurate value of D is impossible to obtain. However, if it is assumed that the Tl atoms are 4 Å apart, that $A_{12}/\hbar = 20$ kHz, and $\langle\Delta\omega^2\rangle^{1/2} = 2\pi\langle\Delta\omega^2\rangle^{1/2} = 91$ kHz (see Sec. VI A for a discussion concerning the calculation of A_{12} and $\langle\Delta\nu^2_{205}\rangle^{1/2}$,

$$D = 1.7 \pm 0.8 \times 10^{-10} \text{ cm}^2/\text{sec},$$

where exchange effects have been taken into account. Note that this number is 10^2–10^3 higher than normal spin-diffusion coefficients encountered in solids—this is due to the inclusion of exchange effects in the calculation of D, which are much more important for thallium nuclei than other nuclei normally encountered in NMR studies.

IV. EXPERIMENTAL

Elemental thallium consists of two naturally abundant isotopes, both of which possess a spin $I = \frac{1}{2}$, and nearly equal gyromagnetic ratios [$\gamma(^{205}\text{Tl}) = 24.57$ MHz/T, $\gamma(^{203}\text{Tl}) = 24.33$ MHz/T]. The primary difference between the two isotopes is in their respective natural abundances, ^{205}Tl being 70.5% abundant, while ^{203}Tl is 29.5% abundant; this has already been shown to be important in its effect upon spin diffusion.

Wide-line measurements were made using a nuclear induction continuous wave spectrometer at 18.57 MHz and at room temperature. An example of the resulting absorption spectrum is shown in Fig. 1.

Relaxation time measurements were made using a MATEC model 515 gated amplifier, a MATEC model 615 broadband receiver, and appropriate auxiliary equipment, arranged in a single-coil, phase-detection system. Temperature regulation was performed by an N_2 gas flow system, flowing

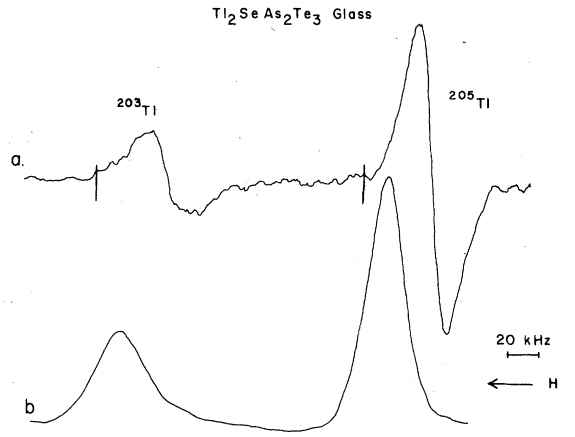

FIG. 1. NMR derivative of the absorption (a) and integrated derivative of the absorption (b) for $Tl_2SeAs_2Te_3$ glass at 18.57 MHz and 297 K.

gaseous N_2 through liquid N_2 to obtain temperatures below room temperature, and through a heat torch for temperatures above room temperature. The temperature measurements were made from a copper-Constantan thermocouple imbedded in the glass which enabled the temperature of the sample to be determined within ±2 K.

Spin-lattice relaxation times T_1 were measured by two methods: (a) inversion recovery[27] ($T_1 \leq 65$ msec), and (b) progressive saturation[28] ($T_1 \geq 65$ msec), while spin-spin relaxation times T_2 were measured by the spin-echo technique.[29] The inversion recovery technique for measuring T_1 uses a 180° pulse to invert the nuclear magnetization, and a 90° pulse (which places the magnetization perpendicular to the applied magnetic field) at a time τ later to sample the magnetization at time τ. For exponential relaxation, the resulting mag-

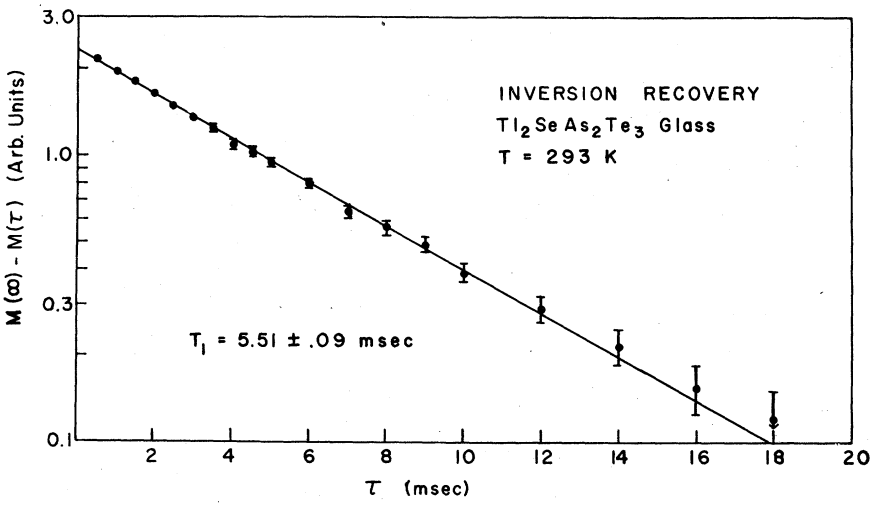

FIG. 2. Resultant magnetization curve, plotted semilogarithmically, for the inversion recovery technique.

netization after the 90° pulse is given by

$$M(\tau) = M(\infty)(1 - 2e^{-\tau/T_1}).$$

The progressive saturation technique for the measurement of T_1 uses a 90°-τ-90-τ . . . pulse sequence, and results in a magnetization after a 90° pulse given by

$$M(\tau) = M(\infty)(1 - e^{-\tau/T_1}).$$

The spin-echo technique for measuring T_2 uses a 90°-τ-180°-τ-echo pulse sequence, the echo height being given by

$$M(\tau) = M(0)\, e^{-\tau/T_2}.$$

An example of the data obtained from the inversion recovery technique is shown in Fig. 2. Since the plot of $\ln [M(\tau) - M(\infty)]$ vs τ is a straight line, the relaxation is exponential within experimental error; this was true for all T_1's and T_2's measured. In all cases T_1 and T_2 were determined using a weighted linear least-square fit of $\ln [M(\infty) - M(\tau)]$ vs τ. The actual error will be greater than indicated in Fig. 2, due to effects mentioned below.

Various errors can come into the T_1 measurement if certain precautions are not taken. In all cases, there is a certain amount of rf leakage that comes directly from the gated amplifier into the receiver. This is only important for $\tau \leq 1$ msec, and can be corrected by subtracting off the purely instrumental effects. The improper setting of the pulse widths will also create an error,[20] though the effect is much more pronounced in the progressive saturation technique than in the inversion recovery technique. For this reason, the inversion recovery method is preferred; however, equipment limitations required that the progressive saturation method be used above $T_1 = 65$ msec. At temperatures where both techniques could be employed, the two methods yielded the same values of T_1, within experimental error. The confidence limits for T_1 were found to be 10% using the inversion recovery technique (for T_1's below 65 msec), and 15% using the progressive saturation technique (for T_1's above 65 msec), while the confidence limits for T_2 were found to be 10%.

TABLE I. Wide-line NMR characteristics of $Tl_2SeAs_2Te_3$ and $Tl_2Se(2As_2Se_3$ glasses).

	$Tl_2SeAs_2Te_3$	$Tl_2Se(As_2Se_3)$
Isotropic chemical shift ($\Delta H/H$)	−0.25% [a]	−0.16% [b]
203 linewidth at 18.57 MHz [$\Delta\nu(^{203}Tl)$]	34.2 kHz	33.9 kHz
205 linewidth at 18.57 MHz [$\Delta\nu(^{205}Tl)$]	22.8 kHz	23.1 kHz
$\frac{\Delta\nu(^{203}Tl)-\Delta\nu(^{205}Tl)}{\Delta\nu(^{205}Tl)}$	0.50	0.47
205 linewidth extrapolated to 0 frequency $\Delta\nu(^{205}Tl)$	9.8 kHz [a]	12.3 kHz [b]
T_2	37 μsec	70 μsec

[a] Reference 11.
[b] Reference 13.

V. RESULTS

A wide line NMR spectrum of ^{203}Tl and ^{205}Tl in $Tl_2SeAs_2Te_3$ glass is shown in Fig. 1, where Fig. 1(a) is the derivative of the absorption and Fig. 1(b) is the integral of Fig. 1(a), displaced slightly to the high-field side in order to get the entire spectrum on the figure. The second moments of the ^{203}Tl and the ^{205}Tl spectra were calculated resulting in $\langle\Delta\nu(^{203}Tl)^2\rangle^{1/2} = 18.2$ kHz and $\langle\Delta\nu(^{205}Tl)^2\rangle^{1/2} = 14.4$ kHz. Other wide line NMR measurements were performed on $Tl_2SeAs_2Te_3$ and $Tl_2Se(2As_2Se_3)$ glasses by Bishop, Taylor, and Mitchell[11,13]; the significant results are summarized in Table I.

The T_1 date for $Tl_2SeAs_2Te_3$ glass plotted versus reciprocal temperature are shown in Fig. 3 for the entire temperature range considered (77 K–425 K),

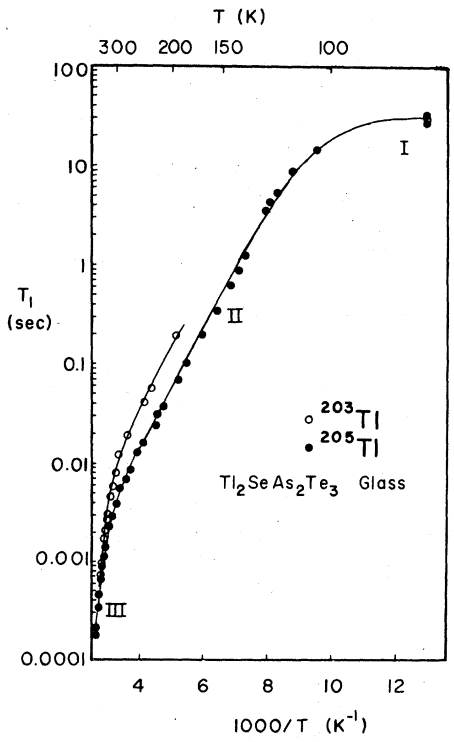

FIG. 3. Spin-lattice relaxation time (T_1) plotted semilogarithmically vs reciprocal temperature for $Tl_2SeAs_2Te_3$ glass, showing all three regions of temperature dependence.

where the highest temperature is well above the glass transition temperature. Clearly, the temperature dependence can be divided into three temperature regions. The low temperature region (region I) is not well characterized, but the data for this region can be fitted to the equation

$$1/T_1^{\mathrm{I}} = K_{\mathrm{I}}\, T^n, \tag{13}$$

where the quantities K_{I} and n are given in Table II. Region II (the intermediate temperature region) is characterized by an Arrhenius temperature dependence of T_1 and an isotope dependence of the prefactor. The data can be fit to the equation

$$1/T_1^{\mathrm{II}} = K_{\mathrm{II}} \exp(-\Delta E_{\mathrm{II}}/kT), \tag{14}$$

where ΔE_{II} is taken from the slope of the data (when plotted as log T_1 vs $1/T$, as is done in Fig. 3), and K_{II}, which is dependent upon the isotope, is the intercept at infinite temperature; values of ΔE_{II} and K_{II} calculated from the data are given in Table II. The high-temperature region (region III) is shown in Fig. 3 and in more detail in Fig. 4; in this region, T_1 is characterized by an Arrhenius temperature dependence, no isotope dependence, and an operating-frequency (or, equivalently, applied-field) dependence that goes as ν_0^2(or H^2). The data can be fit to the equation

$$1/T_1^{\mathrm{III}} = (K_{\mathrm{III}}/\omega^2) \exp(-\Delta E_{\mathrm{III}}/kT), \tag{15}$$

where K_{III} and ΔE_{III} are given in Table II, and $\omega = 2\pi\nu_0$.

TABLE II. Constants obtained for Eqs. (21), (22a)–(22c), and (23) by fitting the NMR data to these equations.

	$Tl_2SeAs_2Te_3$	$Tl_2Se(2As_2Se_3)$
K_{I} ($\sec^{-1} T^{-n}$)	0.00045	0.0020
n	~1	1.1
K_{II} (^{203}Te) ($\sec^{-1}$)	1.15×10^4	1.15×10^6
K_{II} (^{205}Te) ($\sec^{-1}$)	2.7×10^4	3.7×10^6
ΔE_{II} (eV)	0.125	0.36
K_{III} ($\sec^{-3}$)	1.0×10^{29}	2.7×10^{39}
ΔE_{III} (eV)	0.70	1.7
E_g (eV)	0.70 [a]	1.5 [b]

[a] Reference 30.
[b] Reference 31.

Similar results are obtained for $Tl_2Se(2As_2Se_3)$ glass. Figure 5 shows the temperature dependence of T_1 in region II. Again, the temperature depen-

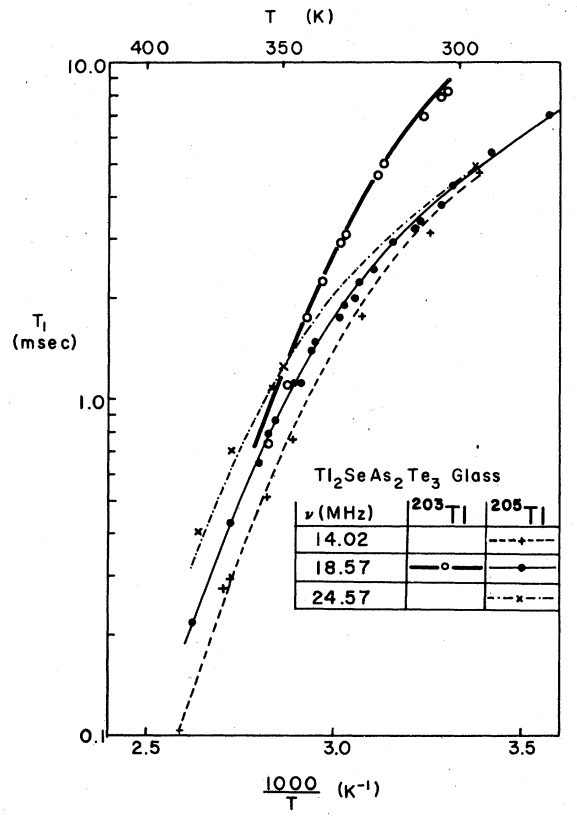

FIG. 4. Spin-lattice relaxation time (T_1) plotted semilogarithmically vs reciprocal temperature for $Tl_2SeAs_2Te_3$ glass at high temperatures (region III) for three different operating frequencies.

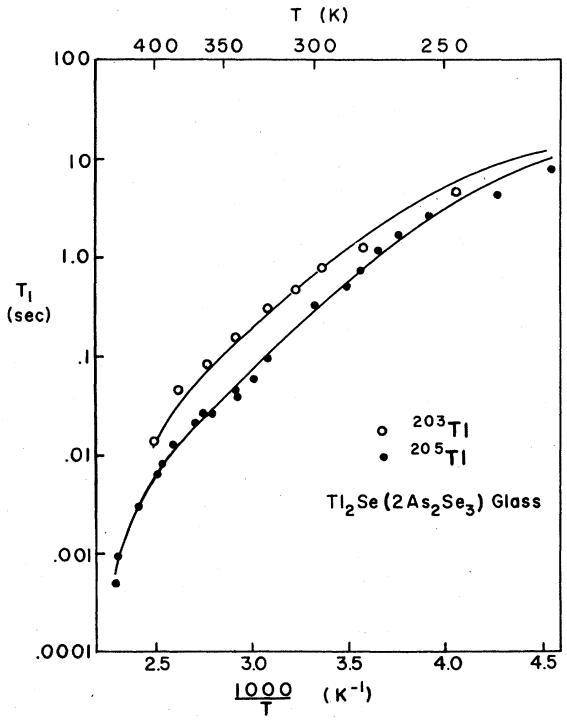

FIG. 5. T_1 plotted vs reciprocal temperature for $Tl_2Se(2As_2Se_3)$ glass for medium temperatures.

dence of T_1 is Arrhenius, while $T_1(^{205}\mathrm{Tl}) \simeq T_1(^{203}\mathrm{Tl})/3.2$; T_1 follows Eq. (15) in this region, where the values of K_{II} and ΔE_{II} are given in Table II. Figure 6 shows an expanded plot of log T_1 vs $1/T$ for region III; again Eq. (15) is obeyed where the values of K_{III} and ΔE_{III} are given in Table II. The data for region I are much more extensive for this glass than for the $Tl_2SeAs_2Te_3$ glass. Figure 7 shows a plot of log T_1 vs log T for region I; as can be seen, Eq. (13) is appropriate for this region, since the points fall, within experimental error, on a straight line. The resulting values of K_I and n are given in Table II.

The curved lines in Figs. 3–6, as well as the numbers quoted in Table II result from a χ-squared fit of the data to Eq. (7) for three regions of temperature dependence, where $1/T_1^I$, $1/T_1^{II}$, and $1/T_1^{III}$ are given by Eqs. (13)–(15), respectively, and where the quantities K_I, K_{II}, K_{III}, η, ΔE_{II}, and Δ_{III} were varied. In this way, the data between two different regions of temperature dependence can be taken into account. As can be seen, the fit is excellent.

The resulting values of T_2 were found to be independent of temperature, isotope, and operating frequency over the temperature region considered. The value of T_2 for $Tl_2SeAs_2Te_3$ glass is 37 μsec, while T_2 for $Tl_2Se(2As_2Se_3)$ glass is 70 μsec.

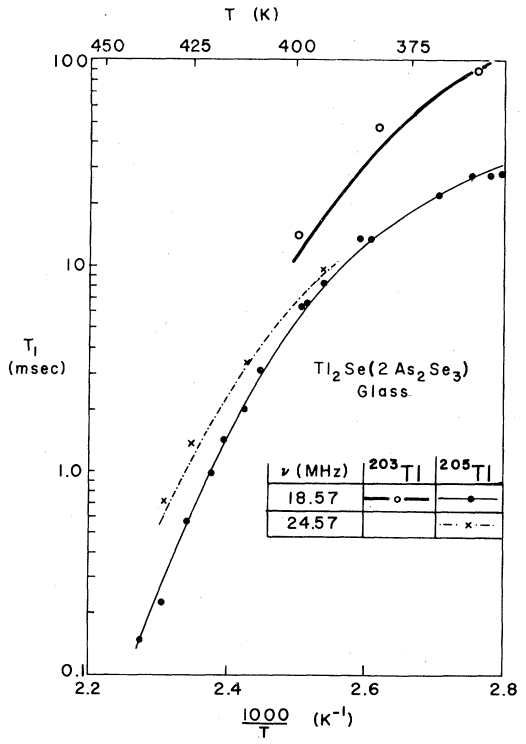

FIG. 6. T_1 plotted semilogarithmically vs reciprocal temperature for $Tl_2Se(2As_2Se_3)$ glass at high temperatures (region III) for two different operating frequencies.

VI. ANALYSIS

A. Wide-line NMR measurements

Four conclusions can be drawn from the wide-line data of Bishop, Taylor, and Mitchell[11,13] and the data presented here.

(a) The isotropic part of the chemical shift ($\Delta H/H$) is large and negative for both glasses; this indicates that the paramagnetic part of the chemical shift dominates and the thallium atoms are covalently bonded.[23]

(b) The linewidth of the ^{203}Tl isotope [$\Delta\nu(^{203}\mathrm{Tl})$] is considerably larger than the linewidth for the ^{205}Tl isotope. This indicates that the exchange interaction is an extremely effective broadening mechanism. Since exchange between like nuclei does not broaden, while exchange between unlike nuclei does, and since ^{205}Tl will have fewer *unlike* neighbors (due to its larger natural abundance) than ^{203}Tl, the exchange interaction will broaden the ^{203}Tl resonance more than the ^{205}Tl resonance. Therefore, the bonding electrons of nearest-neighbor thallium atoms overlap one another as is required for the exchange interaction to be effective (i.e., there are either Tl-Tl pairs in the glass, or next-nearest-neighbor thallium bonding such as Tl-Se-Tl, within the glass network; this sort of behavior is seen also in thallium-containing oxide glasses[32]).

(c) The field dependence of the linewidth indicates that the anisotropic part of the chemical shift is large (~0.12% for $Tl_2SeAs_2Te_3$ glass).[11] This indicates that the electron cloud about the thallium atoms is far from spherical, which is consistent with the covalent nature of the thallium bonding.

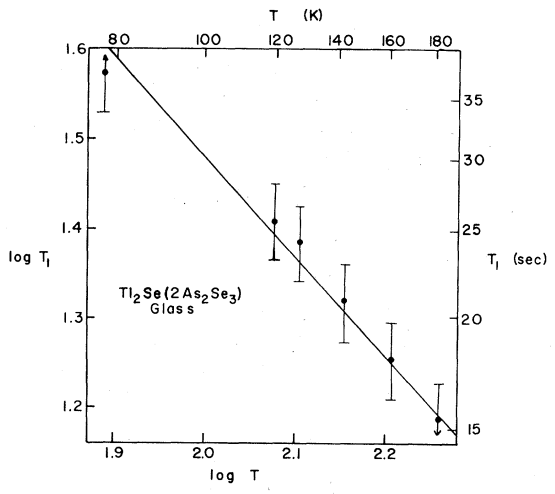

FIG. 7. Log T_1 vs log T for $Tl_2Se(2As_2Se_3)$ glass at low temperatures (region I).

(d) The temperature dependence of the wide-line spectra for the $Tl_2SeAs_2Te_3$ glass indicates that the linewidth is independent of temperature up to $T = 395$ K, which is well above the glass transition temperature ($T_g = 360$ K for this glass); therefore motional narrowing is not observed, even at 395 K, which is 35 K above T_g.

From the wide-line results presented here, and from other thallium NMR studies, it can be concluded that the exchange interaction is a primary broadening mechanism. The accurate determination of A, the exchange coupling constant, is very difficult, even in crystalline materials where the crystalline structure is known. In amorphous materials, the problem is even greater, since the precise positions of the atoms are not known. However, if certain approximations are made, a value of A can be obtained from the second moment values presented in Sec. V. The second moment of the resonance line is given by[25]

$$\langle \Delta\nu^2 \rangle = \langle \Delta\nu^2 \rangle_{cs} + \langle \Delta\nu^2 \rangle_{ex} + \langle \Delta\nu^2 \rangle_{dd} , \tag{16}$$

where $\langle \Delta\nu^2 \rangle_{cs}$ is the contribution from the anisotropic chemical shift (this will be proportional to the square of the applied magnetic field), $\langle \Delta\nu^2 \rangle_{ex}$ is the contribution from the exchange interaction, and $\langle \Delta\nu^2 \rangle_{dd}$ is the contribution from the dipolar and pseudodipolar interactions (the latter two are grouped, since to a first approximation, it is impossible to separate them). The contribution to Eq. (16) from the chemical shift can be eliminated by extrapolating the results to zero field. Note that the results in Table I are quoted in terms of linewidth, not second moments. To convert linewidth to second moments, the ratio of the second moment to the linewidth was taken: $\sqrt{\langle \Delta\nu^2(^{205}\mathrm{Tl}) \rangle} / \Delta\nu(^{205}\mathrm{Tl}) = 0.63$; therefore $\sqrt{\langle \Delta\nu^2(^{205}\mathrm{Tl}) \rangle} = 6.2$ kHz and $\sqrt{\langle \Delta\nu^2(^{203}\mathrm{Tl}) \rangle} = 17.1$ kHz (note that the chemical shift will be the same for both isotopes). This process of taking the ratio for the determination of the zero-field second moment is not very accurate, as the ratio will depend on the character of the resonance line shape (for example, the ratio will be 0.5 for a Gaussian line shape, and ∞ for a Lorentzian); if the line shape changes as a function of applied field, the above analysis will be in error. Since exchange broadening is more important for the ^{203}Tl isotope than for the ^{205}Tl isotope, the chemical shift broadening will be correspondingly less important. Therefore, a more accurate value of A will be obtained from the ^{203}Tl data. The second moment for the exchange interaction is given by[25]

$$\langle \Delta\nu^2 \rangle_{ex} = \frac{1}{3N} \frac{S(S+1)}{\hbar^2} \sum_{ij'} A_{ij'}^2 , \tag{17}$$

where N is the total number of thallium atoms in the sample, the primed subscripts indicate ^{203}Tl nuclei, and the unprimed subscripts indicate ^{205}Tl nuclei. If it is now assumed that only nearest neighbors contribute, and that the exchange coupling constant is the same for all pairs of unlike nuclei, then ($A_{ij} = A_{ex}$),

$$\langle \Delta\nu^2 \rangle_{ex} = [z(1-f)/4h^2] A_{ex}^2 , \tag{18}$$

where f is the natural abundance and z is the number of nearest neighbors. The fact that the linewidth of ^{203}Tl is much greater than the linewidth of ^{205}Tl indicates that the exchange character of the indirect interaction is much greater than the pseudodipolar character, and that the contribution to the second moment from the pseudodipolar (as well as the purely dipolar) interaction can be ignored. If it is assumed that $z = 4$, the quantity A_{ex} can be determined from Eq. (18) and from the second moment of the ^{203}Tl isotope:

$$|A_{ex}|/h = \nu_{ex} \simeq 20 \text{ kHz} .$$

A similar value is obtained for the $Tl_2Se(2As_2Se_3)$ glass. This value compares favorably with values of A_{ex} obtained in other thallium-containing compounds (e.g., $\nu_{ex} = 17.5$ kHz in thallium metal, and $\nu_{ex} = 12$ kHz in Tl_2O_3).[25]

B. Low-temperature T_1 measurements (region I)

The temperature dependence of T_1 in region I is characterized by

$$1/T_1^{\mathrm{I}} = K_{\mathrm{I}} T^n , \tag{13}$$

where $n \sim 1-1.1$. Furthermore, T_1^{I} is frequency and isotope independent.

A possible relaxation mechanism that could result in the above temperature dependence is the Raman-like excitation and deexcitation of disorder modes[33,34] known to exist in amorphous materials. The transition rate T_1^{-1}, to the lowest order in perturbation theory, is given by[34]

$$T_1^{-1} = 2 \times \frac{2\pi}{\hbar^2} \int_0^{E_m} \frac{|H_{\mathrm{I}}|^2 \rho_D^2(E)}{1 + \cosh(E/k_B T)} dE , \tag{19}$$

where H_{I} is the matrix element connecting a disorder mode to the nucleus, $\rho_D(E) = \rho_{D,0} E^{\eta/2}$ is the density of disorder modes, $\frac{1}{2}\eta$ being positive and much less than unity, E is their energy splitting, and E_m is the maximum energy difference between two disorder modes. In Refs. 33 and 34, H_{I} was taken to be the quadrupole interaction, the nuclei being coupled to the lattice via the fluctuations of the electric field gradient at the site of the nucleus. This mechanism is not possible in the present

case, since neither thallium isotope possesses an electric quadrupole moment, and hence does not interact with the electric field gradient. However, H_I can be magnetic in origin, the nucleus being coupled to the lattice via fluctuating dipole coupling, fluctuating chemical shifts, or exchange coupling. If it is assumed that the matrix element of the coupling, H_I, is independent of the energy separating the two interacting disorder modes, then the temperature dependence of T_1^{-1} is given by Eq. (13), where $n = 1 + \eta$, where η is small. Clearly, this relaxation mechanism gives the same temperature dependence as the relaxation in region I. The rate of relaxation via disorder modes, however, is determined by the matrix element H_I, as well as $\rho_{D,0}$; the determination of these quantities relies upon detailed information of the disorder modes and their coupling to the resonant nucleus, which is not presently available. Therefore a detailed analysis of the prefactor K_I is not yet possible.

C. Intermediate-temperature T_1 measurements (region II)

The temperature dependence of region II can be expressed as

$$1/T_1^{II} = K_{II} \exp(-\Delta E_{II}/kT) , \tag{14}$$

where K_{II} is isotope dependent and frequency independent. This region has been treated briefly in Ref. 17 for $Tl_2SeAs_2Te_3$ glass.

The dependence of K_{II} on the isotope of thallium means that the relaxation process in region II relies on spin diffusion (see Sec. III). This indicates that the sample must be inhomogeneous with respect to the nuclear magnetic relaxation process: there must be at least two different types of regions in the sample, (a) regions of type 1, where the nuclei relax directly with the lattice, and (b) regions of type 2, where the nuclei relax indirectly, communicating with the nuclei in regions of type 1 via spin diffusion.

A model for nuclear relaxation via spin diffusion can now be constructed on the basis of the two types of regions mentioned above. Several assumptions must be made.

(a) Relaxation in the regions of type 1 is much faster than in regions of type 2 (if this were not the case, T_1 would be independent of D, and therefore of isotope).

(b) Spin diffusion follows the simple diffusion equation:

$$D\nabla^2 m(r,t) = \frac{\partial m}{\partial t}(\vec{r},t) , \tag{20}$$

where D is the diffusion constant and m is the local nuclear magnetization (or spin temperature). This assumption is nontrivial in the sense that applying the simple diffusion equation above to the case of spin diffusion[18] requires that the sample possess a periodic lattice. Since the sample is a glass, there is a distribution of all local structural parameters, i.e., there is no long-range structural order. Additionally, the sample is placed in a magnetic field, which makes diffusion along the magnetic field about four times more efficient than diffusion perpendicular to the magnetic field.[35,36]

(c) States in regions of type 1 are stable for a time on the order of the duration of the experiment ($\sim 3T_1$). Evidence supporting this assumption will be presented later.

(d) The regions of type 1 are of uniform size and evenly distributed throughout the glass.

(e) If the localized state is paramagnetic, there will be a region about the localized state (defined by a radius b_0) within which the resonance line is broadened beyond obserability and another region (defined by radius b_1) within which the spin diffusion process is no longer effective (see Refs. 35–37). These additional complications are ignored in the present treatment. Since the localized state is diffuse, and since the exchange interaction is responsible for line broadening as well as the spin diffusion process, the two radii, b_0 and b_1 will be nearly equal to the radius of the localized state (r_0), and the two effects can be ignored.

Two cases can be treated mathematically for the model presented above. The two are distinguishable on the basis of the relative sizes of the separation of the localized states (regions of type 1), R, and the diffusion length, $L(=\sqrt{DT_1})$: case 1, $L \gg R$; case 2, $L \lesssim R$.

Case 1 ($L \gg R$) treats the situation where the local magnetization can diffuse into the vicinity of several regions of type 1 before actually being relaxed. This is similar to the case treated by Abragam, in which he obtained

$$1/T_1 = 4\pi N r_0 D , \tag{21}$$

where r_0 is a scattering length and N is the density of localized states. Equation (21) was derived in Ref. 18 for the case where the localized states were paramagnetic impurities, but the assumptions made were such that the present problem is also described by Eq. (21), if the quantity r_0 is now taken to be the radius of the regions of type 1.

Case 2 ($L \lesssim R$) occurs when the local mangetization diffuses slowly, such that it can interact with only one localized state in the duration of the experiment. The diffusion equation [Eq. (20)] can be solved for this case subject to three boundary conditions:

$$m(r_0,t) = m_1^0\,, \tag{22a}$$

$$\frac{\partial m(\frac{1}{2}R,t)}{\partial r} = 0\,, \tag{22b}$$

$$m(r,0) = 0\,. \tag{22c}$$

The first boundary condition [Eq. 22(a)] results from the requirement that nuclei in regions of type 1 relax much faster than nuclei in regions of type 2 (the quantity m_1^0 is just the equilibrium local magnetization of regions of type 1). The second boundary condition [Eq. (22b)] results from the requirement that the outer boundary of a region of type 2 occurs midway between two adjacent localized states, and therefore there will be no net diffusion of magnetization across the boundary. The third boundary condition [Eq. (22c)] results from the requirement that the spin system is saturated at time $t = 0$. It is further assumed that all boundaries are spherical; therefore the regions of type 2 will exist between a sphere of radius r_0, and a sphere of radius $\frac{1}{2}R$. These assumptions clearly represent an oversimplification, but if we are concerned only with order of magnitude estimates, the model will yield meaningful results. The solution of Eq. (20) subject to the boundary conditions of Eq. (22a–c) is presented in the Appendix, and yields

$$1/T_1 = 3r_0D/(\tfrac{1}{2}R - r_0)^3\,. \tag{23}$$

If it is now assumed that $r_0 \ll \frac{1}{2}R$ and $1/N = 4\pi \times [\frac{1}{3}(\frac{1}{2}R)^3]$, then

$$1/T_1 = 4\pi r_0 DN\,, \tag{24}$$

a result which is equivalent to that obtained for case 1. Thus, there is no distinction between the two cases for $\frac{1}{2}R \gg r_0$.

Since a value of D has been calculated [$D = (1.7 \pm 0.8) \times 10^{-10}$ cm^2/sec, see Sec. III], a value of N, the density of localized centers, can be determined from either Eq. (21) or (23), if one assumes a value of r_0.

Figure 8 shows N {or equivalently R, since $1/N = 4\pi[\frac{1}{3}(\frac{1}{2}R)^3]$} and L, the diffusion length, as a function of temperature, plotted for several different cases. The values of N are calculated using Eq. (21) or (23) and the values of K_{II} and E_{II} obtained from the data. Curve 3 shows N vs T for $Tl_2SeAs_2Te_3$ glass, where r_0 has been chosen to be 30 Å, using Eq. (21); curve 4 is similar, except that Eq. (23) is used. Note that curve 3 is considerably above curve 4 at higher temperatures, but, at lower temperatures, the two curves merge. At high temperature, $L < R$ (L is given by curve 1),

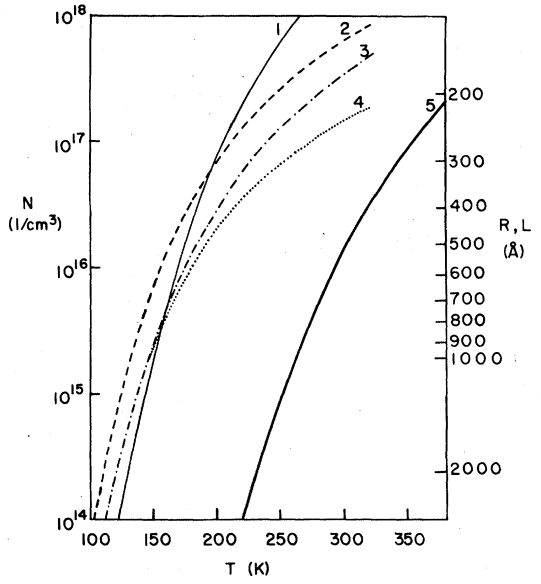

FIG. 8. Density of localized states (N), the separation of the localized states (R), and the spin-diffusion length (L) plotted vs temperature for various circumstances. The quantity N is to be read off the left scale, while R and L are to be read off the right scale. Curve 1: $Tl_2SeAs_2Te_3$ glass, L. Curve 2: $Tl_2SeAs_2Te_3$ glass, N and R calculated from Eq. (23), $r_0 = 10$ Å. Curve 3: $Tl_2SeAs_2Te_3$ glass, N and R calculated from Eq. (21), $r_0 = 30$ Å. Curve 4: $Tl_2SeAs_2Te_3$ glass, N and R calculated from Eq. (23), $r_0 = 30$ Å. Curve 5: $Tl_2Se(2As_2Se_3)$ glass, calculated using Eq. (23), $r_0 = 10$ Å.

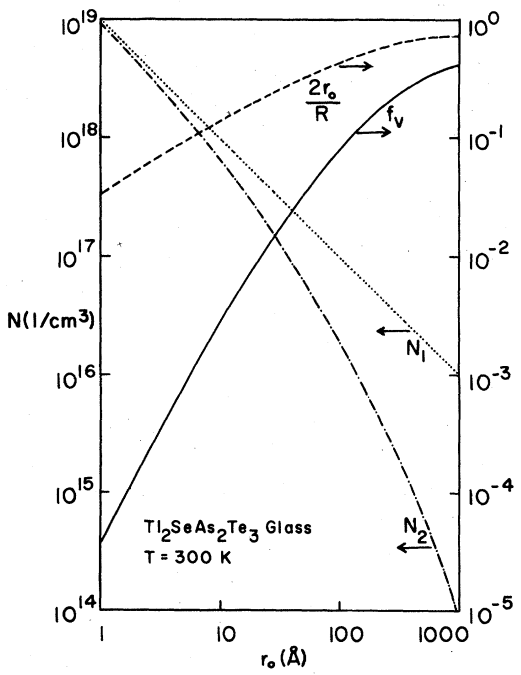

FIG. 9. Density of localized states [N_1 from Eq. (21), N_2 from Eq. (23)], fractional volume of regions of type A ($f_v = 8r_0^3/R^3$), and $2r_0/R$ plotted logarithmically vs log r_0. The left-hand scale is for N_1 and N_2, while the right-hand scale is for f_v and $2r_0/R$.

which violates the conditions for the use of Eq. (21); at lower temperatures, the conditions for the use of Eq. (21) are valid, but Eq. (23) yields the same result. Therefore, Eq. (23) can be employed over the entire temperature range. Curves 2 and 5 show the calculated values of N and R for $Tl_2SeAs_2Te_3$ glass (curve 2) and $Tl_2Se(2As_2Se_3)$ glass (curve 5), using Eq. (23) and assuming $r_0 = 10$ Å.

Though it is not possible to calculate the value of r_0, it is possible to place realistic limits on its value. Figure 9 shows the calculated values of N vs assumed values of r_0 at 300 K for $Tl_2SeAs_2Te_3$ glass. N_1 refers to the density calculated from Eq. (21), while N_2 refers to the density calculated from Eq. (23). As is expected, the two calculated values merge as $r_0 \to 0$ [this is the assumption made in going from Eq. (23) to Eq. (24)]. More importantly, we can also calculate, as a function of r_0, the fraction of the total volume occupied by the localized states ($f_v = 8r_0^3/R^3$); this is shown in Fig. 9 as the curve labeled f_v. Now if f_v were greater than 0.05, the curve $\ln[M(\infty) - M(\tau)]$ vs τ would have two detectable line segments, a line segment of low values of τ with a larger slope (and hence shorter T_1) resulting from direct relaxation within the localized state, and a line segment at larger values of τ, with a longer T_1, resulting from indirect relaxation, via spin diffusion (compare Fig. 2); this was not observed, which indicates from Fig. 9 that $r_0 < 70$ Å. It is possible that a very fast T_1 process would not be observed if T_1 were less than the minimum observed τ (in the case $\tau_{min} = 30$ μsec). However, since $T_1 \geq T_2$ (compare Table I), this possibility can be discounted. From Eq. (23), this indicates that $N(300\text{ K}) > 4 \times 10^{16}$ centers/cm^3 in $Tl_2SeAs_2Te_3$ glass.

D. High-temperature T_1 measurements (region III)

The temperature dependence of T_1 in the high-temperature region is characterized by

$$1/T_1^{III} = (K_{III}/\omega^2)\exp(-\Delta E_{III}/kT)\,, \tag{15}$$

where K_{III} is independent of isotope. Therefore, spin diffusion is not a limiting factor in this region. Additionally, T_2 is independent of temperature and the linewidth of $Tl_2SeAs_2Te_3$ glass does not change until the glass is well into the molten phase.

The ω^2 frequency dependence indicates that the relaxation mechanism may be due to some motion of the thallium atoms. This is also reasonable in that this region occurs around the glass transition temperature in both glasses. The resulting form of T_1 for a motional process is given by[20,38]

$$1/T_1 \sim \langle b_{loc}^2 \rangle \tau/(1+\tau^2\omega^2)\,, \tag{25}$$

where τ is some correlation time, and b_{loc}^2 is the mean-square fluctuation amplitude of the local fields. For large $\omega\tau$, if it is assumed that

$$\tau = \tau_0 e^{\Delta E/kT},$$
$$1/T_1 \propto \langle b_{loc}^2/\omega^2\tau_0 \rangle e^{-\Delta E/kT}, \tag{26}$$

which is of the form observed experimentally. Furthermore a T_1 minimum will be observed at $\omega = 1/\tau$, where

$$(1/T_1)_{min} \propto \langle b_{loc}^2/2\omega \rangle\,. \tag{27}$$

If the fluctuating fields are due to the dipole-dipole interaction (see Sec. II), then[29,38]

$$\langle b_{loc}^2 \rangle \sim (\gamma_1\gamma_2 h/r_{12}^3)^2 I(I+1)\,. \tag{28}$$

If it is now assumed that $r_{12} = 4.0$ Å, then $(T_1)_{min} \sim 2$ sec at $\nu_0 = 20$ MHz. This indicates that the T_1 relaxation in region III is not due to dipole-dipole motional effects, since the smallest T_1 observed is 100 μsec.

If the fluctuating fields are due to chemical shift anisotropy, then[20]

$$\langle b_{loc}^2 \rangle \sim \gamma^2 H_0^2 \delta_{cs}^2\,, \tag{29}$$

where H_0 is the applied magnetic field and δ_{cs} is a measure of the chemical shift anisotropy. But $H_0 = \gamma\omega$, which requires that T_1 be independent of frequency for large τ, contrary to experiment. Therefore, the T_1 relaxation in region III cannot be due to a modulation of the anisotropic portion of the chemical shift interaction.

The pseudodipolar part of the indirect interaction could also be responsible for relaxation in this region. If the relaxation is motional fluctuations of B_{12}, then $\langle b_{loc}^2 \rangle \sim B_{12}^2$. If the pseudodipolar coupling constant is 15 times the classical dipole-dipole strength, then $(T_1)_{min} = 5$ msec. This is again too large, and so the pseudodipolar part of the indirect interaction is not responsible for the relaxation.

A fourth possibility for the relaxation mechanism in this region is the exchange coupling between unlike nuclei. The fluctuating field comes from the time dependence of the coupling between I and S, where the relaxation time is given by[18]

$$1/T_1^{(1)} = \tfrac{8}{3}\pi^2(A_{ex}^2/h^2)S(S+1)\{\tau_e/[1+(\omega_I-\omega_S)^2\tau_e^2]\}\,, \tag{30}$$

where τ_e is the chemical exchange correlation time, I refers to the resonant nuclei and S refers to off-resonant nuclei. For this relaxation mechanism to be effective ("scalar relaxation of the

first kind"), either $1/T_1$ or $1/\tau_e$ must be much larger than $2\pi\nu_{ex}$.[18] Since $2\pi A/h = 2\pi\nu_{ex} = 125$ kHz, clearly $1/T_1$ is not much larger than $2\pi\nu_{ex}$, but $1/\tau_e$ may be. "Scalar relaxation of the second kind" requires that the T_1 of the spin S be much smaller than T_1 of spin I; this is clearly not the case, since K_{III} [of Eq. (15)] is independent of isotope. Therefore, if the relaxation is exchange coupled, it must be scalar relaxation of the first kind.

A comparison of the values obtained from Eq. (3c) indicates that exchange coupling is in all probability the correct relaxation mechanism. Clearly, $(\omega_I - \omega_S)\tau_e \gg 1$ (since there is an ω^2 dependence of T_1). If a particular value of τ_e is assumed, then a value of ν_{ex} can be calculated. Two methods were used: (a) the smallest value of T_1 observed was chosen as $(T_1)_{min}$ (this will yield a lower bound on ν_{ex}) and (b) $(T_1)_{min}$ was chosen to be T_2, the temperature being the intersection point of an extrapolation of the ln T_1 vs $1/T$ curve and ln T_2; since $T_1 \geq T_2$, this will yield a maximum value of ν_{ex}. At $(T_1)_{min}$, $\omega_I - \omega_S = 1/\tau_e$, and the following results are obtained:

$$Tl_2SeAs_2Te_3, \quad 19 < \nu_{ex} < 48 \text{ kHz},$$

$$Tl_2Se(2As_2Se_3), \quad 20 < \nu_{ex} < 31 \text{ kHz}.$$

In all cases, $1/\tau_e \gg 2\pi\nu_{ex}$, so this condition for scalar relaxation of the first kind is satisfied. Note that the results presented above agree with the calculated value $\nu_{ex} = 20$ kHz (see Sec. VI A). Considering the possible sources of error, the agreement is remarkable, and certainly is consistent with the proposition that the nuclear relaxation in region III is due to scalar relaxation of the first kind.

VII. DISCUSSION

Thus far, the nature of the localized ralaxation centers in the regions of type 1 has not been discussed. This has been unnecessary since the analysis does not depend upon the nature of these localized centers—only that they be localized, stable and very efficient relaxation centers. These facts, coupled with the Arrhenius temperature dependence of $1/T_1$ (and hence N), strongly indicate that these localized relaxation centers are in fact localized electronic states in the gap of amorphous semiconductors.

As discussed in Sec. II, unpaired electrons with substantial s character (such as conduction electrons in metals) can create nuclear relaxation via the Fermi contact interaction as well as a Knight shift. Since H_{Fc} contains γ_e ($\sim 10^3\gamma_n$), this type of relaxation is very efficient. It has also been shown by Warren[15,16] that localization of electrons in liquid semiconductors can enhance the nuclear spin-lattice relaxation relative to that which would be expected from the Korringa relation (the Korringa relation states that $T_1(\Delta H/H_0)^2 = \text{const}/T$, where $\Delta H/H_0$ is the Knight shift). This enhancement, as well as the enhancement due to localized electronic states in the gap of amorphous semiconductors, stems from the requirement that the electrons must be at the nuclear site in order to effect relaxation. The more an electron is localized, the more time it spends at the nuclear sites within the special domain of the localized state, and the more chance it has to relax the nucleus.[39] Therefore, localized electronic states will be extremely effective relaxation centers for nuclei in their immediate vicinity.

It has been assumed above [Sec. VI, assumption (c)] that the localized states must also be stable for the duration of the experiment. Pfister and Scher have performed drift mobility measurements on As_2Se_3 glass and determined that there is a large distribution of trap times (from 10^{-6} to 1 sec) in this glass.[40] If the localized states observed here are the trapped electrons observed in the drift mobility measurements, the trap times are indeed reasonable and many of the localized states would be stable for the duration of the experiment.

Therefore, it is reasonable to identify the localized spin-lattice relaxation centers in the regions of type 1 as localized electronic gap states with a large amount of s character, since (a) the temperature dependence indicates that the localized relaxation centers are thermally activated with activation energy less than $\frac{1}{2}E_g$, (b) localized electronic states would be extremely efficient relaxation centers, and (c) the stability requirement is satisfied by the localized trapped electronic states in the gap of amouphous semiconductors.

Additional insight concerning the nature of the localized centers giving rise to spin-lattice relaxation can be gained from a consideration of the activation energy, ΔE_{II}, obtained by fitting Eq. (14) to the data of region II in Figs. 3 and 5. As mentioned previously, the values given in Table II are in each case considerably less than the thermal activation energy for intrinsic electrical conduction ($\frac{1}{2}E_g$). This fact and the localized nature of the centers as indicated by the occurrence of spin diffusion in the relaxation process are consistent with thermally activated occupation of localized states or traps lying well below (above) the conduction (valence) band edge; these occupied traps then function as localized relaxation centers. Under this interpretation the activation process differs from the usual thermal

activation of carriers from localized gap states or traps into delocalized conduction or valence-band states as inferred from thermally activated conductivity measurements. The latter process represents the thermal *emptying* of the localized states, while we are apparently observing the thermally activated *occupation* of deep lying localized states. If it is assumed that in a one-electron picture the thermal activation is to either an isolated localized level or the lowest energy of a band tail of localized states extending into the gap, the depth of this level below the conduction band edge or extent of the band tail could be given by $\frac{1}{2}E_g - \Delta E_{II}$ or 0.225 eV for $Tl_2SeAs_2Te_3$ and 0.35 eV for $Tl_2Se(2As_2Se_3)$. It is these energies which should coincide with the thermal activation energies derived from extrinsic transport measurements on chalcogenide glasses. For example: Andriesch and Kolomiets[41] have reported a localized level (trapping level) lying 0.23 eV above the top of the valence band in $Tl_2SeAs_2Te_3$, on the basis of thermally stimulated current measurements.

Alternatively, if one chooses to describe the nuclear spin-lattice relaxation process in terms of the doubly occupied or two-electron localized gap states proposed by Anderson[5] (see also Street and Mott,[6] Kastner, Alder, and Fritzsche,[7] and Ngai, Reinecke, and Economou[8]), the activation energy presumably represents the energy required to convert a doubly occupied gap state into a singly occupied localized state and a delocalized carrier in one of the bands of extended states. The singly occupied localized state which is thermally generated is, of course, the localized spin-lattice relaxation center.

If, in fact, localized electronic states are responsible for the relaxation, then they would be expected to have unpaired spins—i.e., they would be paramagnetic. However, no ESR or magnetic susceptibility has been observed resulting from localized electronic states in the gap of pure chalcogenide glasses in the equilibrium state. Presumably, the absence of observable paramagnetism is attributable to the low density of these thermally activated centers expected in the relatively wide gap chalcogenide glasses that have been studied. The minimum number of spins that magnetic susceptibility measurements can observe is about 10^{15} spins/cm^3 at 4 K; at 300 K, the lower limit of observability increases to 10^{17} spins/cm^3. As can be seen from Figs. 8 and 9, it might be possible to observe a localized state contribution to the magnetic susceptibility in the narrow gap $Tl_2SeAs_2Te_3$ glass at 300 K, and in $Tl_2Se(2As_2Se_3)$ glass at somewhat higher temperatures. However, the numbers that are predicted are on the borderline of observability—one may or may not see the signal. ESR measurements might also be used to observe these localized states; however, it is not clear how delocalization will affect the ESR line. As r_0 is increased above ~10 Å, the ESR line should broaden, due to scattering, and as many as 10^{18} spins/cm^3 would not produce an observable signal. In addition, the large interaction of the spins of the s-like localized electronic states with the thallium nuclei, as evidenced by the observed spin-lattice relaxation, indicates that a large hyperfine interaction could also arise which would seriously broaden the ESR. The ESR measurements have been performed in pure $Tl_2SeAs_2Te_3$ glass, and no signal due to localized states was observed[42]; therefore, a lower limit of $r_0 \geq 10$ Å seems reasonable. Correspondingly, a maximum value can be placed on N(300 K) of 6×10^{17} spins/cm^3 in $Tl_2SeAs_2Te_3$ glass (see Fig. 9). Note that corrections of Eqs. (22a–c) (see the Appendix) have not been employed. For small values of $2r_0/R$, these corrections are negligible.

This upper limit coupled with the estimated lower limits calculated in Sec. VI place N and r_0 for $Tl_2SeAs_2Te_3$ glass within the ranges (at 300 K) $4\times10^{16} < N < 6\times10^{17}$ spins/cm^3, 70 Å $> r_0 >$ 10 Å. Similar limits for $Tl_2Se(2As_2Se_3)$ glass at room temperature can be established, but, since the density is smaller (see Fig. 9), the limits are much broader; we obtain (at 300 K) $8\times10^{13} < N < 1.4\times10^{16}$ spins/cm^3, 500 Å $> r_0 >$ 10 Å.

VIII. SUMMARY

The temperature dependence of the spin-lattice relaxation time (T_1) for thallium nuclei has been studies in two thallium-containing chalcogenide glasses [$Tl_2SeAs_2Te_3$ and $Tl_2Se(2As_2Se_3)$]. These data indicate that there are three regions of distinctly different temperature dependence which are characteristic of different spin-lattice relaxation mechanisms. At low temperatures, the relaxation is most likely due to a Raman excitation and de-excitation of the disorder modes characteristic of amorphous materials. At intermediate temperatures, the relaxation process relies upon spin diffusion which demonstrates that the relaxation mechanism is provided by localized states; in addition, the exponential temperature dependence of T_1 in this intermediate range reveals that the density of these localized relaxation centers in thermally activated. At high temperatures, the relaxation is most likely due to exchange-coupled scalar relaxation of the first kind.

A model is presented for the nuclear relaxation in the intermediate temperature regime. From the analysis of this model, it is possible to place a

lower limit on N, the density of localized centers which contribute to the spin-lattice relaxation process in the glass, and an upper limit on r_0, the characteristic radius of the localized centers. From ESR, a lower limit on r_0 is obtained, which results in an upper limit on N. The most reasonable interpretation of the relatively small activation energy, ΔE_{II}, which is obtained by fitting the model to the data, is that the localized relaxation centers are localized electronic gap states or traps lying well below (above) the conduction (valence) band edge, whose occupation is thermally activated. When occupied, these localized electronic states provide an efficient spin-lattice relaxation mechanism for adjacent nuclei through the Fermi contact interaction. These efficiently relaxed localized volumes or regions then provide the relaxation mechanism for the remainder of the sample volume through the spin-diffusion process.

ACKNOWLEDGMENTS

The authors would like to thank P. C. Taylor, U. Strom, T. L. Reinecke, and D. L. Mitchell for many helpful discussions. One of us (G.E.J.) would like to thank the National Research Council for financial support.

APPENDIX: SOLUTION OF THE DIFFUSION EQUATION FOR CASE 2

Assume that the diffusion equation [Eq. (20)] holds, subject to the boundary conditions in Eqs. (22a)–(22c). Furthermore, assume that the boundaries are spherical. Therefore, the local magnetization, m (or spin temperature), in a region of type 2, the region between the sphere of radius r_0 and the sphere of radius $\frac{1}{2}R$, will be given by[43]

$$m(r,t) = \frac{2}{r}\sum_{m=1}^{\infty}(1-e^{-D\beta_m^2 t}) \times\left(\frac{\beta_m^2+4/R}{(\tfrac{1}{2}R-r_0)(\beta_m^2+4/R^2)-2/R}\right) \times\frac{m_1^0 r_0}{\beta_m}\sin\beta_m(r-r_0)\,, \tag{A1}$$

where β_m are the solutions of the transcendental equation,

$$\tan\beta_m(\tfrac{1}{2}R-r_0) = \beta_m(\tfrac{1}{2}R)\,, \tag{A2}$$

D is the diffusion constant and m_1^0 is the equilibrium local magnetization. In an NMR experiment, we are interested in the total magnetization in a region of type 2, M_2, which is given by

$$M_2 = \int_{r_0}^{R} m(r,t)4\pi r^2\,dr\,. \tag{A3}$$

The integral can be performed, yielding,

$$M_2 = m_1^0\sum_{m=1}^{\infty} V_m(1-e^{-D\beta_m^2 t})\,, \tag{A4}$$

where

$$V_m = \frac{16\pi r_0^2}{R\beta_m^2},\quad \frac{1}{\sin^2\beta_m(\tfrac{1}{2}R-r_0)-2r_0/R}\,. \tag{A5}$$

The quantity V_m is in units of volume, and goes to $V_0 = (4\pi)/3(\frac{1}{8}R^3 - r_0^3)$ as $2r_0/R \to 0$; in fact V_m/V_0 is the fraction of the contribution that the mth term makes to the sum in Eq. (A4). For example, for $2r_0/R = 0.4$, $V_1/V_0 = 0.94$; since the ratios $2r_0/R$ shown in Fig. 9 will be less than 0.4 for the limits considered (see Sec. VII), a reasonable approximation is to ignore all but the $m = 1$ term. Therefore

$$1/T_1 = D\beta_1^2\,, \tag{A6}$$

where β_1 is the smallest solution of Eq. (A2). If $\tan\beta_1(\frac{1}{2}R-r_0)$ is expanded in a Taylor series, where only the first two terms are kept, then

$$1/T_1 \cong 3r_0 D/(\tfrac{1}{2}R-r_0)^2\,. \tag{A7}$$

The use of Eq. (A7) will introduce an error in the calculated values of N ($=\frac{1}{6}\pi R^3$), tending to make N too large. The error in N is dependent upon the ratio $2r_0/R$, being 52% for $2r_0/R = 0.3$, and 13% for $2r_0/R = 0.1$.

---

*Present address: Solid State Division, Oak Ridge National Laboratory, Oak Ridge, Tenn. 37830.

[1]N. F. Mott and E. A. Davis, *Electronic Processes in Non-Crystalline Materials* (Clarendon, Oxford, 1971).

[2]*Amorphous and Liquid Semiconductors*, edited by J. Tauc (Plenum, New York, 1973).

[3]M. H. Cohen, H. Fritzsche, and S. R. Ovshinsky, Phys. Rev. Lett. 22, 1065 (1969).

[4]E. A. Davis and N. F. Mott, Philos. Mag. 22, 903 (1970).

[5]P. W. Anderson, Phys. Rev. Lett. 34, 953 (1975).

[6]R. A. Street and N. F. Mott, Phys. Rev. Lett. 35, 1293 (1975).

[7]M. Kastner, D. Adler, and H. Fritzsche, Phys. Rev. Lett. 37, 1504 (1976).

[8]K. L. Ngai, T. L. Reinecke, and E. N. Economou, Phys. Rev. B 17, 790 (1978).
[9]M. H. Brodsky and R. S. Title, Phys. Rev. Lett. 23, 581 (1969).
[10]S. C. Agarwal, Phys. Rev. B 7, 685 (1973).
[11]S. G. Bishop, P. C. Taylor, and D. L. Mitchell, J. Non-Cryst. Solids 8–10, 106 (1972).
[12]S. G. Bishop and P. C. Taylor, Solid State Commun. 11, 1323 (1972).
[13]S. G. Bishop and P. C. Taylor, Phys. Rev. B 7, 5177 (1973).
[14]S. G. Bishop, *Proceedings of the Fifth International Conference of Amorphous and Liquid Semiconductors* (Taylor and Francis, London, 1973), p. 997.
[15]W. W. Warren, Phys. Rev. B 3, 3708 (1971).
[16]W. W. Warren, Phys. Rev. B 6, 2522 (1972).
[17]G. E. Jellison, Jr. and S. G. Bishop, Phys. Rev. Lett. 40, 1204 (1978).
[18]A. Abragam, *The Principles of Nuclear Magnetism* (Clarendon, Oxford, 1961).
[19]C. P. Slichter, *Principles of Magnetic Resonance* (Harper and Row, New York, 1963).
[20]D. Shaw, *Fourier Transform N. M. R. Spectroscopy* (Elsevier, New York, 1976).
[21]W. E. Lamb, Phys. Rev. 60, 817 (1941).
[22]N. F. Ramsey, Phys. Rev. 86, 243 (1952).
[23]S. Hafner and N. H. Nachtrieb, J. Chem. Phys. 40, 2891 (1964).
[24]W. D. Knight, *Electron Paramagnetism and Nuclear Magnetic Resonance in Metals, Solid State Physics, Vol. 2,* edited by Seitz and Turnbill (Academic, New York, 1956), pp. 93–136.
[25]N. Bloembergen and T. J. Rowland, Phys. Rev. 97, 1679 (1955).
[26]N. Bloembergen, Physica 15, 386 (1949).
[27]R. C. Vold, J. S. Waugh, M. P. Klein, and D. E. Phelps, J. Chem. Phys. 48, 3831 (1968).
[28]S. Alexander and A. Tzalmona, Phys. Rev. 138, A845 (1965).
[29]E. L. Hahn, Phys. Rev. 80, 580 (1950).
[30]D. L. Mitchell, P. C. Taylor, and S. G. Bishop, Solid State Commun. 9, 1833 (1971).
[31]Based on luminescence measurements.
[32]L. W. Panek and P. J. Bray, J. Chem. Phys. 66, 3822 (1977).
[33]M. Rubinstein, H. A. Resing, K. L. Ngai, and T. L. Reinecke, Phys. Rev. Lett. 34, 1444 (1975).
[34]T. L. Reinecke and K. L. Ngai, Phys. Rev. B 12, 3476 (1975).
[35]I. J. Lowe and D. Tse, Phys. Rev. 166, 279 (1968).
[36]D. Tse and I. J. Lowe, Phys. Rev. 166, 292 (1968).
[37]H. E. Rorschach, Jr., Physica 30, 38 (1964).
[38]N. Bloembergen, E. M. Purcell, and R. V. Pound, Phys. Rev. 73, 679 (1948).
[39]N. Bloembergen, Physica 20, 1130 (1954).
[40]G. Pfister (private communication).
[41]A. M. Andriesh and B. T. Kolomiets, Sov. Phys. Solid State 5, 1063 (1963).
[42]P. C. Taylor (private communication).
[43]M. N. Ozisik, *Boundary Value Problems of Heat Conduction* (International Textbook, Scranton, 1968).